ANNALS of Faculty Engineering Hunedoara – International Journal of Engineering
ISSN: 1584 - 2665

SQUEEZE-FILM LUBRICATION OF THE HUMAN ANKLE JOINT: A SIMPLIFIED ANALYTICAL MODEL DURING WALKING

Alessandro RUGGIERO, Roberto D'AMATO

University of Salerno, Department of Mechanical Engineering, ITALY

Abstract
The aim of this paper is to propose an analytical approximate squeeze-film lubrication model of the human ankle joint for a quick assessment of the synovial pressure field and the load carrying due to the squeeze motion, considering both normal and pathological behaviour. The model starts from the theory of *boosted lubrication* for the human articular joints lubrication (Walker, et al., 1968; Maroudas, 1969) and takes into account the fluid transport across the articular cartilage using the Darcy's equation to depict the synovial fluid motion through a porous cartilage matrix. The human ankle joint has been assumed as cylindrical enabling motion in the sagittal plane only. The proposed model is based on a modified Reynolds equation; its integration allows obtaining a quick assessment on the synovial pressure field showing a good agreement with those obtained numerically by other Authors (Hlavacèk, 2000). The analytical integration allows the closed form description of the synovial fluid film force and the calculation of the gap thickness.
Key Words: Biotribology, Synovial Pressure Field, Fluid Film Force

1. INTRODUCTION

In the last years there is increasing recognition of the importance of the tribological mechanisms in biomechanics and particular practical interest are devoted to the lubrication of human synovial joints modeling, such as ankle hip and knee joints. It is well known that synovial joints act as mechanical bearings (biobearings) (Walicki et al., 2000) that facilitate the work of the musculoskeletal machine. Depending on the joint location, they may be the spherical bearings—such as hip joints, the quasi-spherical bearings—such as shoulder joints, the quasi-cylindrical bearings—such as knee, elbow, or ankle joints.

Synovial joints are structured from a pin which is a bone head and a sleeve which is an acetabulum. The pins and sleeves are covered with cartilage which constitutes the structure with antifriction properties. The cartilage structure on the pin surface is more compact than that one on the sleeve surface and it should be modeled in many cases as a porous layer. Articular cartilage is a layered medium composed of several structural zones (Lane & Weiss, 1975): superficial, middle and deep. The superficial zone of the normal cartilage is the most distinct and reaches up to 200 μm. Its upper most layer, only about 3 μm thick, is called lamina splendens and is made of non-banded, randomly arranged fine collagen filaments of 4-12nm in diameter. Below this layer there are sheets of a well-identified period, each sheet with predominantly parallel, banded collagen fibrils, their diameter increasing with depth.

Articular cartilage is elastic, fluid-filled, and backed by a relatively impervious layer of calcified cartilage and bone. This means that load-induced compression of cartilage will force interstitial fluid to flow laterally within the tissue and to surface through adjacent cartilage. As that area, in turn, becomes load bearing, it is partially protected by the newly expressed fluid above it.

Biobearings, in general, are lubricated by a synovial fluid which is—in general—a non-Newtonian fluid, but in some cases it can be considered as Newtonian. (Hlavacèk, 1994; Sep & Kucaba-Pietal, 2007). Normal synovial fluid is clear or yellowish; its functions are nutrition and lubrication of cartilage, load bearing, and shock absorption.

In the last years, the research on synovial joints has focussed on two aspects: to investigate on the fundamental lubrication processes occurring in natural joints, and to development of artificial, replacement joints. Mathematical models of human joints serve to predict quantities which are difficult to measure experimentally, and to simulate changes to the physiological conditions.

With particular reference to the human ankle joint, many researchers has been involved in the modeling of the mechanics of joint lubrication, proposing sophisticated models that involve complex numerical algorithms in order to obtained the desired solution. (Hlavacèk, 1994, 2000, 2005). Many theories are based on the hypothesis of *boosted lubrication* (Walker et al., 1968). This lubricating mechanism presupposes that the solvent component of SF (considered as a mixture of two incompressible fluids, a viscous-macromolecular complex of hyaluronic acid-protein and the other ideal-and small-solute-water) flows into the pores of the articular cartilage (solid-liquid biphase mixture) consists of a cartilaginous matrix postulated (filled by a homogeneous isotropic ideal interstitial fluid made of water and small solutes) flattened during the squeeze-action film, so that the concentration of the complex macromolecular acid - hyaluronic protein, present in the SF increases until it reaches a limit value. At this point the film fluid is rapidly depleted and, over the majority of contact between the surfaces, the formation of a film of synovial gel fixed, which prevents the contact, acting as a boundary lubricant if sliding motion between the two articular surfaces prior to the arrival of the new SF. Naturally during walking, the presence of a fluid film for lubrication of the ginglimo angular, ensured by the cyclical nature of the load (Medley et al.,1984), which enables the complete filtering of the ideal fluid through the cartilage of the SF and thus the formation of the gel synovial.

The aim of this paper is to propose a simple analytical squeeze-film lubrication model of the human ankle joint in order to obtain a quick assessment of the fluid film force acting in the articulation by using an analytical solution of the fluid dynamic problem. With this purpose the fluid transport across the articular cartilage has been modeled using the Darcy's equation to depict the synovial fluid motion through a porous cartilage matrix.

2. METHODS

2.1 Human ankle joint geometry and assumptions

According with the hypothesis of literature (Medley et al.,1983) the human ankle joint can be considered as cylindrical, where the motion is allowed only in the sagittal plane; the coupling model is assumed by two infinite rigid circular cylinders (subchondral bone) in the internal contact (a cylinder encased in a cylindrical cavity), covered with thin layer (articular cartilage) of uniform thickness; the lower (talar) articular surface is supposed stationary while the upper (tibial) surface is assumed to have pure squeeze motion $\dot{e}$ (t) with in half a newtonian SF film. The last assumption was justified by Hlavacèk (Hlavacèk, 1996a) which found that the effect of increased viscosity of the normal SF for low shear rates does not influence the fluid film thickness for entraining velocities encountered in walking; it follows that the SF in the ankle joint behaves as Newtonian during walking.

The figure 1 shows the model and the coordinates x, y position in the direction tangential, and radial in the synovial film. It is assumed that the ankle is loaded in the y direction in the plane of symmetry by a load W (t) [N / m], as occurs during walking. The movement occurs in the x-y plane. Articular surfaces move along y. The surface with its centre at x = 0 is bounded with the edges at x = ±a in which the synovial pressure is assumed to be equal to zero. Only the symmetric case is considered in this paper allowing the obtained analytical results the generalization to the others non-symmetrical configurations. For cartilage the linear mixture model (Mow et al., 1980) could be adopted, where the linear (small deformation) homogeneous and isotropic elastic porous cartilage matrix is considered with the ideal interstitial fluid, flowing due to the fluid pressure gradient through the porous matrix.

The adopted gap geometry is qualitatively confirmed by some numerical investigation made by the Authors on real plain radiograph images and on real computed axial tomography data (TAC) (Figure 2).

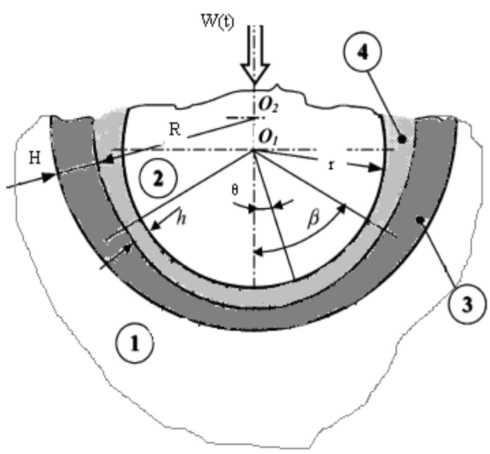

Figure 1 : Human ankle joint geometry

Figure 2: Radiograph images of the Human ankle joint: side view

Starting from TAC data, by using first the Hounsfield unit scale it has been possible to make a threshold of talar and tibial surface. By interpolating the obtained points it has been possible to reconstruct the shape of the surfaces.

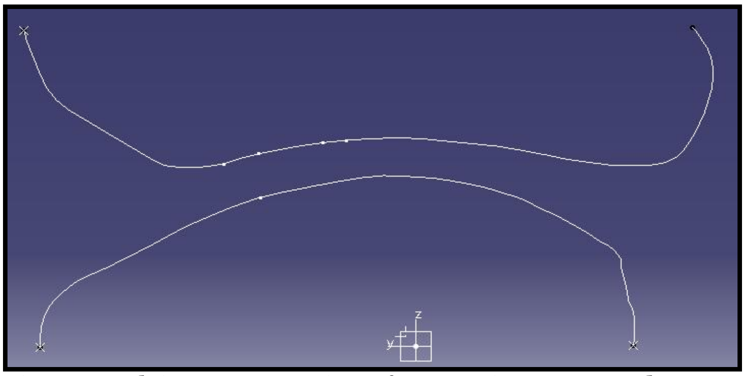

Figure 3 : Plain representation of contact in correspondence of the middle x-y plane

The plain representation of them, in correspondence of the middle x-y plane (figure 3), confirm the adopted geometry.

2.2 Mathematical model

The thickness of the gap of two infinite circular cylinders can be written as (Matthewson, 1981):

$$h(x,t) = \tilde{h}(t) - 2u(x,t) - 2\hat{h}$$

where $\tilde{h}(t)$ is the SF film thickness including cartilage surfaces, u(x) is the entrapment in the vertical direction of the articular surface and $\hat{h}$ is the thickness of the cartilage surfaces; u(x) can be evaluated through the approximation due to Armstrong and Mattheson (Armstrong, 1986; Mattewson, 1981). In order to evaluate the displacement component due to cartilage deformation they considered the constitutive equations of the latter, linear elastic material, related to the cartesian plane x_i (i = 1,2,3) transversely isotropic with the axis x_3. If there are no restrictions on the component ε_{ij}, it is possible to get σ_{ij} the form:

$$\begin{bmatrix} \sigma_{11} \\ \sigma_{22} \\ \sigma_{33} \\ \sigma_{13} \\ \sigma_{23} \\ \sigma_{12} \end{bmatrix} = \begin{bmatrix} C_{11} & C_{12} & C_{13} & 0 & 0 & 0 \\ C_{21} & C_{22} & C_{23} & 0 & 0 & 0 \\ C_{31} & C_{32} & C_{33} & 0 & 0 & 0 \\ 0 & 0 & 0 & 2\mu_{13} & 0 & 0 \\ 0 & 0 & 0 & 0 & 2\mu_{13} & 0 \\ 0 & 0 & 0 & 0 & 0 & 2\mu_{12} \end{bmatrix} * \begin{bmatrix} \varepsilon_{11} \\ \varepsilon_{22} \\ \varepsilon_{33} \\ \varepsilon_{13} \\ \varepsilon_{23} \\ \varepsilon_{12} \end{bmatrix}$$

with:

$$C_{11} = E_1(1 - \nu_{31}^2 E_1 / E_3)/(1 + \nu_{21})\Delta$$

$$C_{12} = E_1(\nu_{21} + \nu_{31}^2 E_1 / E_3)/(1 + \nu_{21})\Delta$$

$$C_{13} = E_1 \nu_{31} / \Delta$$

$$C_{33} = E_3\left[1 + 2\nu_{31}^2 E_1 / (E_3 / \Delta)\right]$$

$$\Delta = 1 - \nu_{21} - 2\nu_{31}^2 E_1 / E_3$$

σ_{ij} (i, j=1,2,3) is the cartilage components stress tensor, ε_{ij} components tensor of small deformations. $\nu_{ij} = -\frac{\varepsilon_{jj}}{\varepsilon_{ii}}$ (i ≠ j) and $E_i = \frac{\sigma_{ii}}{\varepsilon_{ii}}$ are the Poisson ratios and Young's modulus with strain due to the uniaxial component σ_{ii}, respectively while μ_{13}, μ_{12} represent the cutting module, with $\mu_{12} = \frac{E_1}{2(1+\nu_{21})}$.

In the case of cylindrical geometry, is possible to evaluate the vertical displacement u(x) of the articular surface as (Halavacèk, 2006):

$$u(x) = \frac{h^3}{3\mu} S_{,xx}$$

In order to obtain an analytical approximate solution for the pressure field, in this paper, the effects of cartilage deformations are neglect. In fact as already reported in the literature, Hlavacek (2002), this condition occurs for light load.

With reference to the scheme in figure 1, under the classical hypotheses of hydrodynamic lubrication, the Reynolds equation for the contact in the case of pure squeeze motion can be written as follows:

$$\frac{\partial}{\partial x}\left(\frac{h^3}{\mu}\frac{\partial p}{\partial x}\right)+\frac{\partial}{\partial z}\left(\frac{h^3}{\mu}\frac{\partial p}{\partial z}\right)=12(W_{ul}) \tag{1}$$

in which the effective velocity component W_{ul} is composed of two terms: Wp is the y-velocity of the talar surface and W_o is the fluid-velocity due to the permeability of the cartilage matrix.

$$W_{ul}=W_p-W_o \tag{2}$$

The W_o component can be calculated by using the Darcy's equation:

$$W_o=\frac{\Phi H}{\mu}\left(\frac{\partial^2 p}{\partial x^2}+\frac{\partial^2 p}{\partial z^2}\right) \tag{3}$$

in which $\Phi = k\mu \;\left[m^2\right]$ is the permeability factor of the cartilage porous matrix and H= $2\,\hat{h}$

$$W_p=\frac{\partial h}{\partial t}$$

By substituting the eq.(3) in the eq.(1) the modified Reynolds equation can be written as follow

$$\frac{\partial}{\partial x}\left[\left(h^3+12\Phi H\right)\frac{\partial p}{\partial x}\right]+\frac{\partial}{\partial z}\left[\left(h^3+12\Phi H\right)\frac{\partial p}{\partial z}\right]=12\mu\frac{dh}{dt} \tag{4}$$

with

$$h(x,t)=\tilde{h}(x,t)-2\hat{h} \tag{5}$$

in which $\tilde{h}(t)$ is the fluid film thickness including the cartilage layers ($\hat{h}$) .

Assuming mono-dimensional pressure in the x direction the equation (4) became:

$$\frac{\partial}{\partial x}\left[\left(h^3+12\Phi H\right)\frac{\partial p}{\partial x}\right]=12\mu\frac{dh}{dt} \tag{6}$$

By using polar coordinates:

$$\frac{1}{R^2}\frac{\partial}{\partial\theta}\left[\left(h^3+12\Phi H\right)\frac{\partial p}{\partial\theta}\right]=12\mu\frac{dh}{dt} \tag{7}$$

with

$$\tilde{h}(\theta,t)=c+e\cos\vartheta$$

where *c* and *e* are respectively the biobearing clearance and eccentricity

The pressure field is obtained by integrating the (7):

$$p=12R^2\mu\dot{e}\int\frac{\sin\theta}{h^3+12\Phi H}\partial\theta+12R^2\mu\dot{e}c_1\int\frac{1}{h^3+12\Phi H}\partial\theta+c_2 \tag{8}$$

with c_1 and c_2 determined by imposing void values of pressure at $\pm\frac{a}{R}=\pm\beta$,

In order to obtain an approximate analytical solution, the (8) has been replaced with the:

$$p=12R^2\mu\dot{e}\int\frac{\sin\theta}{\left[h(\theta)+12\Phi H-6\Phi e\right]^3}d\theta+12R^2\mu\dot{e}c_1\int\frac{1}{\left[h(\theta)+12\Phi H-6\Phi e\right]^3}d\theta+c_2 \tag{9}$$

in which has been substituted the term $h(\theta)^3+12\Phi H$ with the well fitting $\left[h(\theta)+12\Phi H-6\Phi e\right]^3$.

The synovial pressure field can be written by integrating the (9) in closed form as:

$$p(\theta)=\frac{12R^2\mu\dot{e}\left[-\frac{1}{c-6(-2+e)\Phi+e\cos\beta^2}+\frac{1}{c-6(-2+e)\Phi+e\cos\theta^2}\right]}{2e} \tag{10}$$

The analytical form of the hydrodynamic pressure allows calculating the fluid film force:

$$f_r=L\int_{-\beta}^{\beta}p(\theta)d\theta \tag{11}$$

By solving analytically the (11) we obtain:

$$f_r = 12R^2 \mu \dot{e} L \left\{ \frac{2(c+12\Phi)\operatorname{arctan}h\left[\frac{(c-e+12\Phi)\tan(\beta/2)}{\sqrt{-c^2+e^2-24c\Phi-144\Phi^2}}\right]}{e\left(-c^2+e^2-24c\Phi-144\Phi^2\right)^{3/2}} - \frac{\frac{\beta}{e}+\frac{(c+12\Phi+e\cos\beta)\sin\beta}{\left(c^2-e^2+24c\Phi+144\Phi^2\right)}}{c+12\Phi+e\cos\beta^2} \right\} \quad (12)$$

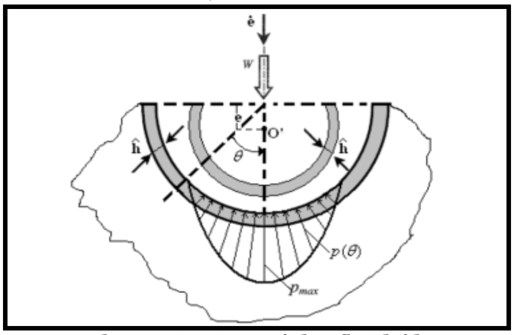

Figure 4: Schematic view of the fluid film pressure

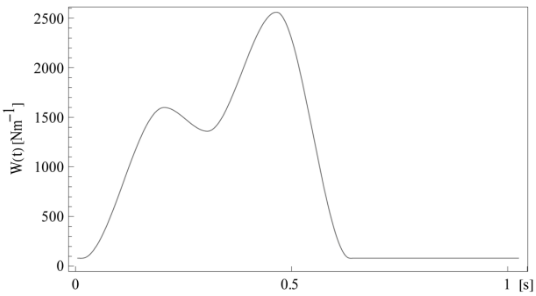

Figure 5: Variation of W(t) in the ankle joint during walking (Hlavacèk, 2005)

By equating the fluid film force (12) to the external load W(t), representing the load cycle during the walking (Hlavacèk, 2005) (Figure 4), and neglecting the others forces acting on the joint, it is possible to write the equilibrium equations for the talar surface in the x-y plane as follow:

$$f_r(e,\dot{e}) = W(t) \quad (13)$$

The (13) represents a non linear differential equation. The numerical solution allows to obtain the time history of the functions e(t) and $\dot{e}$ (t).

3. RESULTS

The numerical integration of the equation (13) has been performed by using a predictor-corrector Adhams method with $e\big|_{t=0} = \bar{h}$, where $\bar{h}$ is the fluid film thickness in absence of the load.

In order to compare the results with those obtained in (Hlavacèk, 2002) the same typical numerical values have been adopted for the calculations (see appendix B).

The calculation of the e(t) function allows to obtain the evolution of the velocity $\dot{e}$ (t) (figure 6) and of the fluid film thickness h(0,t) (figure 7) during the imposed load (walking).

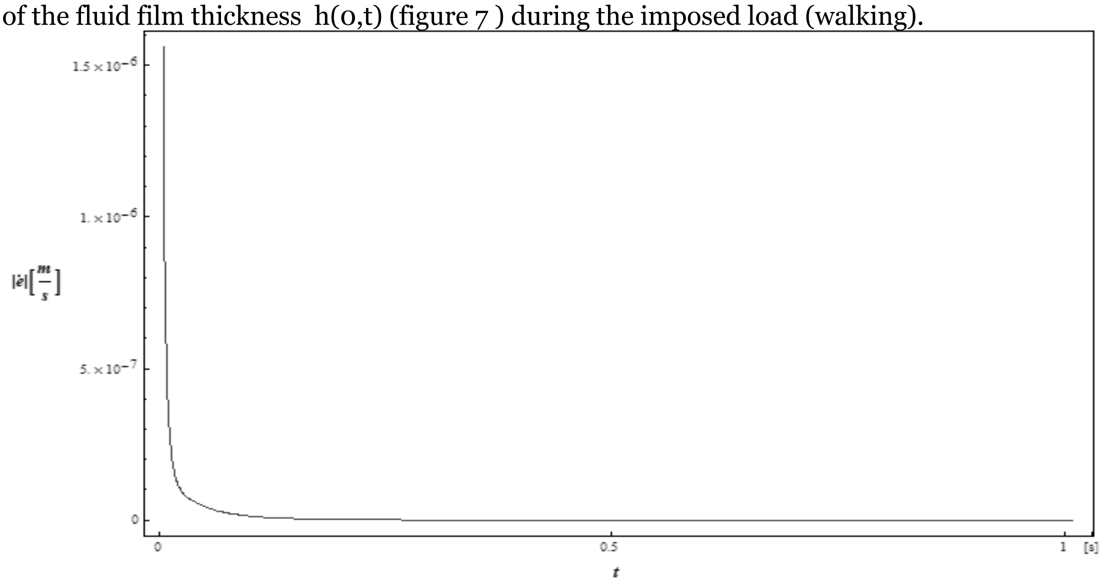

Figure 6: Variation of $\dot{e}$ (t) in the ankle joint during walking

Was also studied the behaviour of the height of the meatus for three different pairs of H and ϕ. For $H = 3\cdot 10^{-3}$, $\Phi = 6\cdot 10^{-17}$ (normal cartilage), for $H = 2\cdot 10^{-3}$, $\Phi = 1\cdot 10^{-17}$ (pathological arthrosis joints) and $H = 1.5\cdot 10^{-3}$, $\Phi = 1.5\cdot 10^{-18}$ (articulation suffers from mild arthrosis) figure 7a.

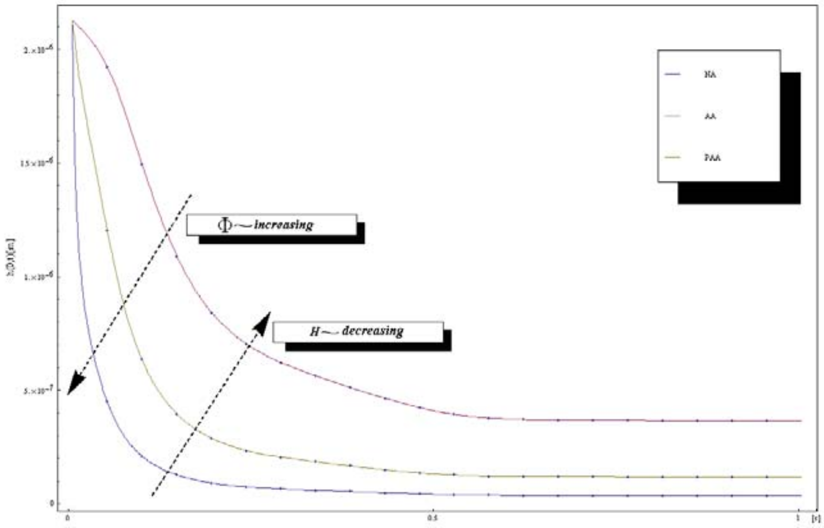

Figure 7: Evaluation of h (0, t) for different values of H and ϕ, NA normal cartilage, PAA arthrosis cartilage pathology, AA and arthrosis cartilage

In figure (8) is shown a typical synovial pressure field by varying the angular coordinate θ and the time during the first 0.05 s of the walking by using the results obtained from the solution of (13).

In figure 9 is shown the different synovial pressure field behavior vs. θ in correspondence of the instant in which the load is applied and for three specific scenarios relative to normal articulation, arthritically and pathologic arthritic joint.

The obtained results have been compared with those reported in Hlavacèk (2000), (2002) and show a good agreement.

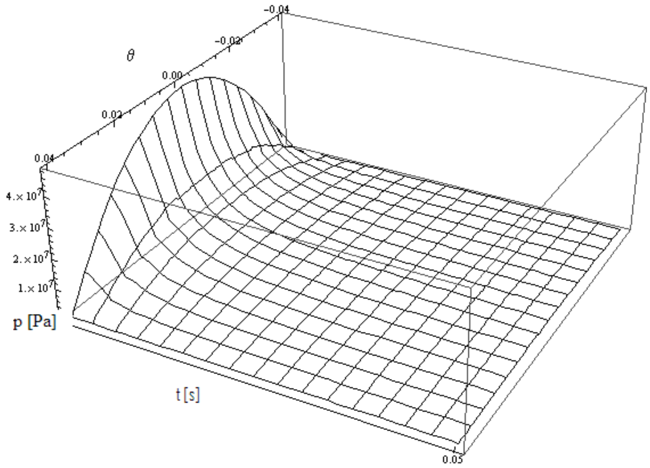

Figure 8: Fluid film pressure field by varying the angular coordinate θ and time

4. DISCUSSION

Observing the obtained results some considerations may be done:

- numerical investigations on real radiographic data confirm the simplified geometry adopted for the mathematical modeling of the synovial joint;
- starting from a simplified model of the human ankle joint, the proposed approach allows to generate the approximate analytical expressions of the pressure field and of the fluid film force acting in a human ankle joint as function of the eccentricity ratio and squeeze velocity;

Due to the adopted hypotheses, the model gives better results in the cases in which it is possible to neglect the effects of the cartilage deformations and of the synovial gel boundary lubricant formation (i.e. low loaded joints).

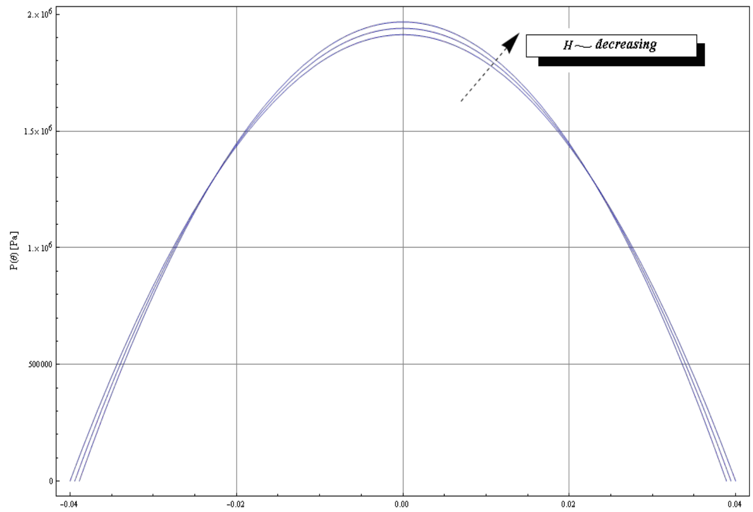

Figure 9: Variation of synovial pressure at the start of the walking for decreasing values of H

The closed form solutions for the synovial pressure field and of the fluid film force are useful in all types of ankle joint dynamic analyses that favor an analytical approach, i.e. in all cases in which the aim is to obtain a better trade-off between accuracy and computational expense for a quick assessment of the forces acting in the synovial joint during a pure squeeze motion and gives a better readability of all the principal geometrical and rheological parameters characterising the synovial joint, allowing to cover not only the individual case, but also the whole class to which the system belongs.

From the analysis of figure 7 and figure 9 it is possible explain the main causes of pain in arthritic joints: figure 7 shows that decreasing values of H produce higher film thickness and local pressure field increase (figure 9), both reason of high stress level in soft tissue (as muscles, ligaments, etc...) and in bone articular surfaces (Talus and tibia).

It should be noted in conclusion that this paper represents a preliminary analysis of a squeezed synovial film and many simplifying assumptions have been adopted in the mathematical modelling in order to receive an analytic solutions. These are, among others, hydrodynamic lubrication, squeeze motion, permeability Darcy's model, rigid cartilage matrix and subchondral bone, newtonian SF. In the literature these assumptions are accepted in some cases, but the Authors hope to obtain in future some experimental verification in order to support the approximate theoretical prediction obtained and/or improve the proposed method.

Appendix A : Nomenclature

a	Tibial length
AC	Articular Cartilage
E	Young's modulus of the cartilage matrix
h(x,t)	Synovial film thickness
ϕ	Permeability of the cartilage matrix
c	Clearance
p(x,t)	Synovial Pressure
q(x,t)	Synovial flow through the cartilage matrix
fr	Synovial fluid film force
$\dot{e}$ (t)	Squeeze velocity
R	$1/R = 1/R_l - 1/R_u$ effective radius of curvature of the contact
R_l, R_u	Radius of curvature of SL and Su
s_l, s_u	Inferior articular surface (thalamus) and upper (tibial)
SF	Synovial fluid
t	Time
u(x,t)	displacement of the articular surface
W(t)	Periodic load for unit of length
μ	Shear modulus of the cartilage matrix
η	Viscosity of synovial fluid

Appendix B : Table numerical values used for the calculations

Parameters	Numerical values	units
a	$14\cdot10^{-3}$	$[m]$
L	$28\cdot10^{-3}$	$[m]$
$\hat{h}$	$1{,}5\cdot10^{-3}$	$[m]$
c	$7{,}25\cdot10^{-7}$	$[m]$
R_e	$3{,}5\cdot10^{-1}$	$[m]$
$R_{l,}$	$22\cdot10^{-3}$	$[m]$
ϕ	$2\cdot10^{-14}$	$\left[\frac{m}{s}\right]$
β	$4\cdot10^{-2}$	rad
μ	10^{-2}	$[Pa\cdot s]$

REFERENCES

[1.] ARMSTRONG, C.G., 1986. *"An analysis of the stress in a thin layer of articular cartilage in a synovial joint". Engrg. Med. 15, pp. 55–61.*

[2.] HLAVACEK, M., 1993a., *"The Role of Synovial Fluid Filtration by Cartilage in Lubrication of Synovial Joints. I. Mixture Model of Synovial Fluid," J. Biomech., 26(10), pp. 1145–1150.*

[3.] HLAVACEK, M., 1993b. *"The role of synovial fluid filtration by cartilage in lubrication of synovial joints—II. Squeeze-film lubrication: homogeneous filtration". Journal of Biomechanics 26, 1151–1160.*

[4.] HLAVACEK, M., 1995. *"The role of synovial fluid filtration by cartilage in lubrication of synovial joints - IV. Squeeze-film lubrication: the central film thickness for normal and inflammatory synovial fluids for axial symmetry under high loading conditions". Journal of Biomechanics, 28, pp. 1199-1205.*

[5.] HLAVACEK, M., 1996a. *"A central film thickness formula for elastohydrodynamic lubrication of cylinders with soft incompressible coating and non newtonian piecewise power-law lubricant in steady rolling motion". Wear, 205, pp. 20-27.*

[6.] *HLAVACEK, M., 2000. "Squeeze-film lubrication of the human ankle joint with synovial fluid filtrated by articular cartilage with the superficial zone worn out". Journal of Biomechanics, 33, pp. 1415-1422.*

[7.] *HLAVACEK, M., 2005. "Squeeze-Film Lubrication of the Human Ankle Joint Subjected to the Cyclic Loading Encountered in Walking". Journal of Tribology, 127, pp. 141-148.*

[8.] *HLAVACEK, M., 2006. "Frictionless contact of two parallel congruent rigid cylindrical surfaces coated with thin elastic transversely isotropic incompressible layers: an analytic solution". European Journal of Mechanics A/Solids 25, pp. 497-508.*

[9.] *HLAVACEK, M., NOVAK, J., 1995. "The role of synovial fluid filtration by cartilage in lubrication of synovial joints - III. Squeeze-film lubrication: axial symmetry under low loading conditions". Journal of Biomechanics, 28, pp.1193-1198.*

[10.] *HLAVACEK, M., VOKOUN.D., 1996b. "Elastohydrodynamic lubrication of cylinders with soft incompressible coating firmly bonded to the substrate". Wear, 197, pp. 1-8.*

[11.] *JAROSŁAW SĘP, ANNA KUCABA PIĘTAL, 2007. "Applications of Finite Element Method in Synovial Joint Numerical Calculations", Proceedings of the International Multiconference on Computer Science and Information Technology, pp. 449 – 455, ISSN 18967094.*

[12.] *LANE, JM, WEISS, C., 1975. "Review of articular cartilage collagen research". Arth Rheum 18: 553-562.*

[13.] *MAROUDAS, A., 1969, "Studies on the Formation of Hyaluronic Acid Films," in Lubrication and Wear in Joints, edited by V. Wright, Sector, London, pp. 124–133.*

[14.] *MATTHEWSON, M.J., 1981. "Axi-symmetric contact on thin compliant coatings". J. Mech. Phys. Solids 29, pp. 89–113.*

[15.] *MEDLEY, J. B., et al., 1983. "Surface Geometry of the Human Ankle Joint". Eng. Med., 12(1), pp. 35–41.*

[16.] *MEDLEY, J. B., et al., 1984. "Transient Elasto-Hydrodynamic Lubrication Models for the Human Ankle Joint," Eng. Med., 13, pp. 137–151.*

[17.] *MOW, et al., 1980. "Biphasic creep and stress relaxation of articular cartilage: theory and experiment". Transactions of ASME, Journal of Biomechanical Engineering 102, 73–84.*

[18.] *WALICKI E. et al 2000. "Mathematical modeling of some biological bearings". Smart Mater Struct. 9 pp. 280-283*

[19.] *WALKER, et al., 1968, "Boosted Lubrication in Synovial Joints by Fluid Entrapment and Enrichment," Ann. Rheum. Dis., 27, pp. 512–520*

ANNALS OF FACULTY ENGINEERING HUNEDOARA
– INTERNATIONAL JOURNAL OF ENGINEERING

Faculty of Engineering Hunedoara,
5, Revolutiei, 331128, Hunedoara,
ROMANIA
http://annals.fih.upt.ro